High temperature corrosion memory in a waste fired boiler – Influence of sulfur

Waste Management 130 (2021) 30–37

Contents lists available at ScienceDirect

Waste Management

journal homepage: www.elsevier.com/locate/wasman

High temperature corrosion memory in a waste fired boiler – Influence of sulfur

M. Dolores Paz [a,*], Julien Phother-Simon [a], Sven Andersson [a,b], Torbjörn Jonsson [a]

[a] Environmental Inorganic Chemistry, Department of Chemistry and Chemical Engineering, Chalmers University of Technology, SE-412 96 Göteborg, Sweden
[b] Babcock & Wilcox Vølund AB, Box 8876, SE-402 72 Göteborg, Sweden

ARTICLE INFO

Article history:
Received 27 November 2020
Revised 28 April 2021
Accepted 3 May 2021
Available online xxxx

Keywords:
High temperature corrosion
Sulfur recirculation
Waste to energy
Corrosion memory

ABSTRACT

The selection of fuel for a Combined Heat and Power (CHP) plant can vary over time. By choosing less expensive fuels, operation costs are reduced, however, cheaper fuels generally increase corrosion maintenance costs. The corrosiveness of different fuels has been studied extensively while how the current corrosion attack is influenced by corrosion history, i.e. previous deposit build-up and oxide scale formation, is less studied. This phenomenon may be referred to as a "corrosion memory" effect (Paz et al., 2017). The present work investigates the influence of addition of sulfur to the fuel on the corrosion memory through air-cooled probes in the Waste-to Energy lines at Måbjerg Energy Center (MEC) in Denmark. The results show a corrosion memory effect, i.e. as initially corrosive environment may increase the subsequent corrosion rate and vice versa.

1. Introduction

The selection of fuel has a great impact on the total budget of a CHP plant. By choosing less expensive fuels (like different fractions of biomass or waste) the profit of the plant can increase greatly. Cheaper fuels are usually more corrosive, and the profit is decreased by increased maintenance costs, due to corrosion. In order to keep these costs low, the steam parameters are normally lowered, resulting in not only lower corrosion rates but also a drop in electrical efficiency. Hence, in order to increase the green electricity production from these corrosive fuels, more effective corrosion mitigation techniques are needed. One promising solution is the Sulfur Recirculation technique (Andersson et al., 2014; Andersson et al., 2019)

The beneficial effect of sulfur addition on high temperature corrosion is well documented (Henderson et al., 2006; Karlsson et al., 2011; Krause et al., 1975; Pettersson et al., 2011; Vainio et al., 2013; Viklund et al., 2009). However, in contrast to other corrosion mitigation techniques based on sulfur containing species, the Sulfur Recirculation avoids the disadvantages of additional residue production by only using the fuel sulfur. The technique aims to change the environment at the superheaters in order to limit the high-temperature corrosion. This is primarily done by decreasing the presence of alkali chlorides. The issue of chlorine and alkali chloride induced corrosion has previously been studied (Gerassimidou et al., 2020; Ma et al., 2020; Meissner et al., 2020; Reddy et al., 2019; Vainio et al., 2019) and different ways to mitigate its effect have been addressed in recent years (Karlsson et al., 2015; Karlsson et al., 2012; Ma, et al., 2020; Meissner, et al., 2020). A successful way to minimize the corrosiveness of alkali chlorides is to sulfate them to corresponding alkali sulfates. This can be done by using elemental sulfur, sulfur-rich additives or by co– combustion with a suitable fuel, e.g. sludge and coal (Henderson et al.; Karlsson et al., 2011; Krause, et al., 1975; Pettersson, et al., 2011; Vainio et al., 2013; Viklund et al., 2009). The presence of sulfur in the fuel changes the flue gas chemistry; alkali chlorides react with SO_2/SO_3 forming alkali sulfates, and chlorine is released as HCl. There are several papers that investigate the gas phase reactions between alkali chlorides and sulfur containing species (Krause, et al., 1975). In addition to these publications, an investigation of the sulfation of solid alkali chlorides (i.e. deposits) and how they affect the corrosion has recently been published (Pettersson, et al., 2011) However, very little is known about the memory effect of a corrosive/less corrosive environment/deposit. Paz et al (Paz, et al., 2017) investigated the corrosion memory influence by introducing a novel scheme that utilized probe exposures in two different boilers, one co-firing biomass and one waste-fired boiler.

The first full scale installation of the Sulfur Recirculation at Måbjerg Energy Center (MEC) in Denmark offers a unique setup to study the corrosion memory effect. The two production lines offers two different environments separated by only 10 m, which

* Corresponding author.
E-mail address: maria.dolores.paz@chalmers.se (M.D. Paz).

https://doi.org/10.1016/j.wasman.2021.05.005
0956-053X/

allows corrosion probes to be moved between these environments during the tests.

The aim is to study the high temperature corrosion memory effect of a commercial stainless steel with air-cooled corrosion probes in a full-scale waste fired boiler using a full-scale installation of the corrosion mitigation technique Sulfur Recirculation.

2. Materials and methods

2.1. The boiler

The Måbjerg Energy Center consists of two waste-fired boilers with a capacity of 2*11 t/h and a straw/woodchips boiler firing 7 t/h. Together they produce 28 MW continuous electrical power and 84 MW district heating. 180.000 t/year of household and industrial waste are treated in the waste lines together with 10.000 t/year of sludge. Both waste-fired lines are operating with the same fuel mix, fed from one bunker. A Sulfur Recirculation system(Andersson, et al., 2019) was installed at Line 1 (L1) shown in Fig. 1. The Sulfur Recirculation installation consists mainly of a storage vessel and dosage system for hydrogen peroxide (H_2O_2), a raw gas analyzer for SO_2, equipment for transport and dosage of sulfuric acid into the furnace. SO_2 is separated in the wet scrubber using H_2O_2, producing a 15-25 wt% H_2SO_4 solution, which is injected into the boiler producing SO_2, thus creating a sulfur loop. The sulfuric acid is sprayed through nozzles with atomization air, which produces a fine mist which evaporates rapidly. The H_2SO_4 dosage rate is controlled by a PID controller, which maintains a fixed SO_2 setpoint downstream of the boiler. The recirculated sulfur will increase the gas concentration of SO_2 in the boiler and decrease the Cl/S ratio of the deposits and ashes, thus lowering chlorine content of the boiler deposits, in order to decrease the high temperature corrosion and the dioxin formation rates as well as dioxin emissions. This produce a setup with the same fuel but different environment for the superheaters in each line. The two different lines are in addition only separated by approximately 10 m and have manholes installed at the superheater position on both lines where air cooled probes could be inserted.

2.2. Probe exposures

The exposures were performed by air cooled probes consisting of two temperature zones, 525 and 450 °C. In order to reach the desired temperature, a cooling system is integrated in the probe. The same probe system was previously used for similar research (Paz, et al., 2017). The corrosion memory effect was investigated by switching the probes between two different lines: the reference line (Line 2, called "Ref") was in normal operating mode, while the Sulfur Recirculation line (Line 1, called "Rec") produced a less corrosive environment by recirculating the sulfur.

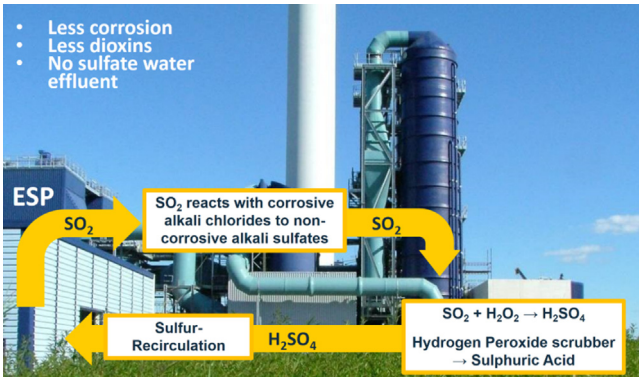

Fig. 1. The flue gas treatment of MEC consists of an ESP (Electrostatic Precipitator), a HCl scrubber and a multistage scrubber for SO_2 removal, dioxin removal using ADIOX and flue gas condensation (Andersson, et al., 2019), reproduced with permission from Detritus journal.

The corrosion memory effect was investigated with four different air-cooled probes:

Two probes stayed in their respective line during the whole 2000 h duration of the exposure: "Ref" was only exposed in the reference line and "Rec" only in the Sulfur Recirculation line.

Two so called "corrosion memory probes" were switched after half of the duration of the exposure: "RefRec" was first exposed for 1000 h in the reference line and then 1000 h in the Sulfur Recirculation line. "RecRef" was exposed the other way around.

The samples were produced as rings in order to fit the air-cooled probes and the material selected for this study was 347H stainless steel (C < 0.1, Cr: 17.0–20.0, Ni: 9.0–13.0, Si < 0.75, Mn < 2.0, Nb: 1.10) exposed at 525 °C. The temperature was controlled by using termocouples and the probes were cooled by using compressed air. The temperature was recorded during the whole process. The measured value was 525 ± 3 °C during the 2000 h exposure.

Highly alloyed sample rings of Sanicro28 were in addition exposed in the same probes in order to investigate the deposit formation in the different lines, i.e. with and without Sulphur Recirculation.

2.3. Analytical techniques

2.3.1. Scanning electron microscopy/energy dispersive X-rays (SEM/EDX)

After the boiler exposure, the samples were cast in epoxy, cut and polished in order to produce a cross-section of the alloy, the corrosion attack and the deposit. The polished cross-sections of the samples were investigated by backscattered (BSE) scanning electron microscopy (SEM). The SEM was equipped with an Energy Dispersive X-ray system enabling analysis of the elemental composition in small areas of the sample. In this study, a FEI 200 Quanta FEG ESEM was used. It is equipped with a field emission electron gun (FEG) and an Oxford Inca energy dispersive X-ray (EDX) system. SEM/EDX was used for imaging, elemental mapping and quantification. An accelerating voltage of 20 kV was used for all analysis.

2.3.2. Material loss measurements

The samples were evaluated by means of metal loss determination. The material thickness prior to exposures were measured with a digital screw micrometer (0.0001 mm resolution). Each sample was measured at 8 different locations by turning the sample ring 45° each time. After the exposure, the sample thickness was measured in the same points with SEM at sample cross sections. The edges of the ring were avoided. The material loss was determined by the difference between the sample thickness before and after the exposures.

2.3.3. Ion chromatography (IC)

The deposits formed were analyzed in detail. The deposits were removed after the 2000 h exposure and analyzed by using Ion Chromatography (IC). To determine water-soluble anions (Cl^-, SO_4^{2-}) in the deposit of the exposed samples, a Dionex ICS-90 system was used. The anions were analyzed with an IonPac AS4A-SC analytic column and 1.8 mM NaHCO3/1.7mMNaHCO3 was used as eluent. The flow rate was 2 mL/min. A representative and known amount of deposit was removed from the samples and dissolved in 100 mL distilled water. A 5 mL sample of this prepared solution was inserted into the IC column in order to know the amount of

chlorine and sulfate ions (ppm). The results are presented as mass percentage (amount of ions/100 g deposit).

3. Results and discussion

3.1. Deposit composition – IC

In order to analyse the deposit composition in the superheater region, some deposit was removed from the air-cooled probes before the removal of the samples. All the deposits were hard and difficult to remove from the probes.

The amount of chlorine and sulphate was determined by means of ion chromatography. Fig. 2 shows the percentage of chlorine and sulphate in the deposit for the reference probes and from the corrosion memory probes.

After 2000 h the reduction of the chlorine is drastic between the Sulfur Recirculation line and the reference line with a 97% reduction of chlorine in the Sulfur Recirculation line. The amount of chlorine in the reference line (Ref) was about 3 wt% and 0,1 wt% in the Sulfur Recirculation deposit (Rec). Regarding the corrosion memory probes which were exposed 1000 h in each line/environment, the dense hard deposits made it very difficult to remove a representative part of the deposit. The first corrosion memory probe is represented as RecRef where the samples were exposed first 1000 h in the sulfur recirculation line and then 1000 h in the reference line. By comparing with the results of the reference exposures, it can be concluded that the RefRec sample has similar amount of chlorine as the deposit on the sulfur recirculation sample (Rec). A similar trend may be observed for the RecRef sample which shows a chlorine content in line with the Reference sample deposit (Ref). This indicates that only the outer part of the deposit was possible to analyse, corresponding this deposit to the last 1000 h of exposure.

Regarding the sulfate, after 2000 h exposure, the amount of sulfur in the Sulfur Recirculation line is approximately 13 wt% and approximately 9 wt% in the reference line as expected. As mentioned above, the hard deposits made it very difficult to take a homogeneous deposit sample for these probes and no significant difference can be found between the RefRec probe, which presents an 8 wt% sulfate, and the RecRef probe with a 9 wt% sulfate. By comparing with the references exposure, it can be seen that only the Rec probe, exposed 2000 h in the sulfur recirculation line, presents a higher amount of sulfate.

3.2. Material loss

The material loss was measured in profile around the sample rings. The flue gas direction is marked with a red arrow, see Fig. 3. All the samples had a higher material loss on the side exposed to the flue gas. This was also the case for the sample exposed 2000 h in the recirculation line (Rec), which showed very little material loss.

The Fig. 4 shows the maximum material loss linearly recalculated to mm/year for the four different exposure conditions. Previous studies with air-cooled probe exposures have shown that the material loss obtained with probe samples is higher than the one obtained when measuring directly on the superheater tubes (Paz et al., 2018; Vinter Dahl et al., 2018). Waste fired boilers operating at similar temperature ranges can generate material loss up to 16 mm/year for commercial stainless steel probe samples (e.g. the grade 304L) when firing industrial waste (Paz, et al., 2017; Paz, 2014). The 347H samples exposed in the reference line during 2000 h presents a material loss of 1,8 mm/year indicating a mild/medium corrosive environment.

Regarding the samples exposed 2000 h in the Sulfur Recirculation line, they reveal a material loss of 0,2 mm/year. This implies a

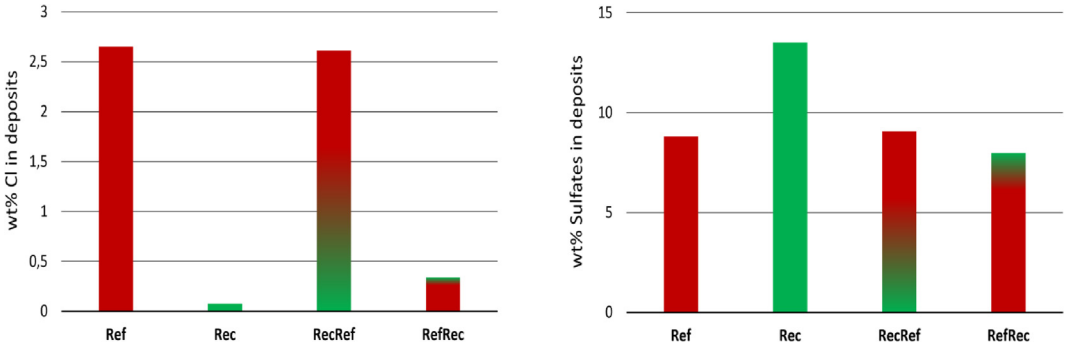

Fig. 2. Chlorine and Sulfates in the probe deposits of the Ref (red), Rec (green), RecRef (green → red) and RefRec (red → green) exposures (wt%). (For interpretation of the references to colour in this figure legend, the reader is referred to the web version of this article.)

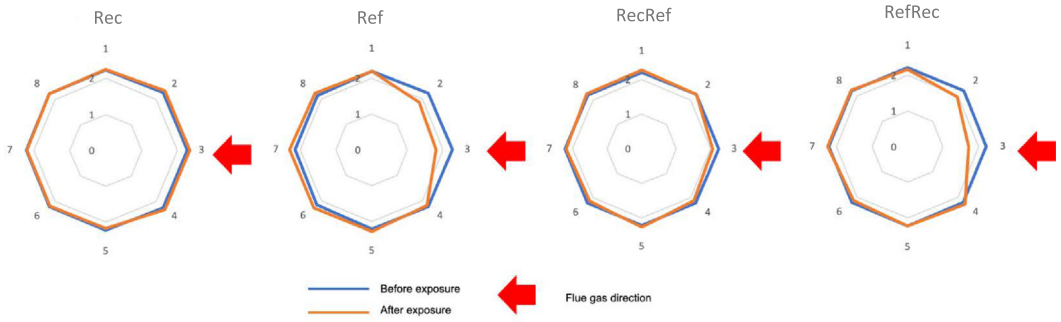

Fig. 3. Material loss after corrosion tests at 525 °C and 2000 h.

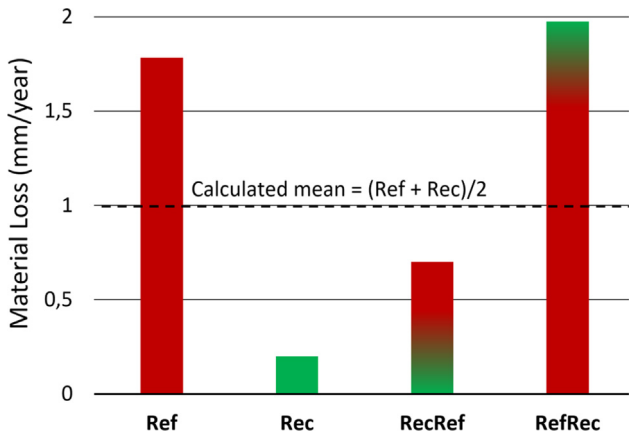

Fig. 4. Maximum material loss (mm/year) of the Ref (red), Rec (green), RecRef (green → red) and RefRec (red → green) exposures. The dashed line represents the calculated mean value of the Rec and Ref exposures. (For interpretation of the references to colour in this figure legend, the reader is referred to the web version of this article.)

reduction of approximately 90% in material loss when running the boiler with sulfur addition. This corrosion value is very low taking into account that material loss in probe exposures in waste/biomass boilers can be in the range of 1 mm/year with same type of stainless steel samples (Paz, 2014) while other sulfur addition techniques resulted in a material loss up to 6 mm/year range at 600 °C (Paz et al., 2018).

The two different lines gives a good possibility to investigate the corrosion memory effect. In order to estimate the combined expected corrosion rate in the mixed exposures the corrosion rate needs to be estimated based on the ref/rec 2000 h exposures. A linear growth rate extrapolated from the different environments would give a predicted material loss of 1,8/2 + 0,2/2 = 1,0 mm/year, i.e. the results (0,7 mm/year) indicate a positive corrosion memory effect of the initial sulfur rich environment/deposit. High temperature corrosion is expected to be diffusion controlled following a parabolic growth rate (Wagner, 1933) predicting a higher value after 1000 h for both the exposures. The samples exposed first 1000 h in the Sulfur Recirculation line (very mild) and then 1000 h in the reference line (mild/medium), results in a material loss of 0,7 mm/year. This is 60% lower material loss than the samples exposed only in the reference line for the same amount of time (2000 h) and lower than the calculated mixed exposure (1,0 mm/year). The samples exposed first 1000 h in the reference line (mild/medium) and then 1000 h in the sulfur recirculation line (very mild), resulted in a material loss of 1,9 mm/year (to be compared with the calculated 1,0 mm/year). This value is in the same range as the samples exposed only in the reference line for the same amount of time indicating a very strong corrosion memory effect when the samples are exposed first in the most corrosive environment. Thus, both the mixed exposures indicate a corrosion memory effect.

These observations agree well with a chlorine-induced accelerated corrosion. The Rec sample exhibited very little material loss compared to the Ref sample. This was also associated with a low chlorine content found in the deposits of the Rec sample due to sulfation of the alkali chlorides. It has been demonstrated that the presence of chlorine generally increases the severity of the corrosion attack. Several mechanisms have been suggested to cause the accelerated corrosion e.g. the active oxidation(Abels and

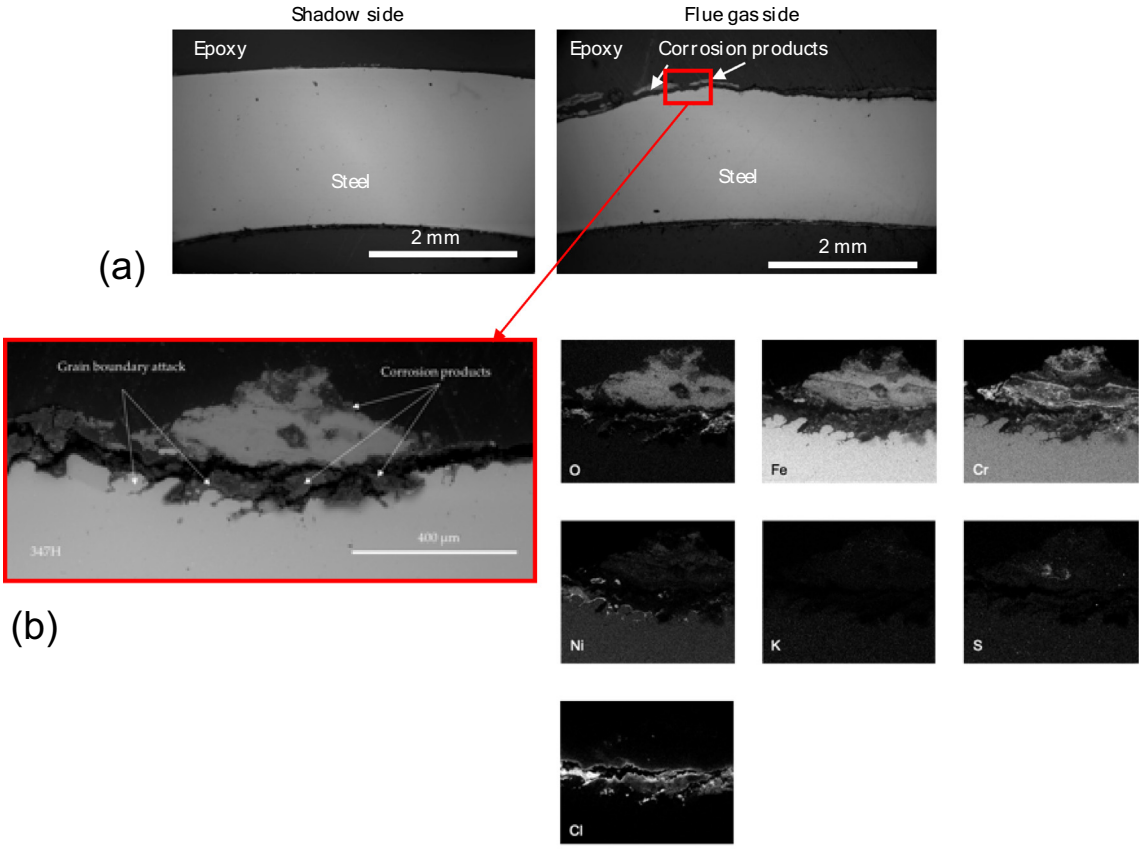

Fig. 5. (a) BSE image showing a low mag cross section of Ref for 2000 h (b) EDX analysis of the flue gas side of Ref for 2000 h.

Strehblow, 1997; Folkeson et al., 2007; Grabke et al., 1995; McNallan et al., 1983; Nielsen et al., 2000; Shinata, 1987; Wang and He, 2002; Zahs et al., 2000) or electrochemical mechanism (Cantatore et al., 2019; Folkeson, et al., 2007; Jonsson et al., 2011). However, the results (see below) indicate the presence of reactive alkali and a breakaway corrosion in all environments even if the Rec sample resulted in a mild corrosion attack.

The corrosion memory sample RecRef was first exposed in the line with Sulfur Recirculation, building the first layers of deposits with a low chlorine content due to the mild environment. After being changed to the reference line (after 1000 h), the deposits from the harsher environment began to stack on top of the previous deposits. Compared to the calculated mean value of material loss expected after 1000 h in each line, the RecRef sample exhibited a lower material loss, see Fig. 4. This could be explained by the first hard layers of deposits with low chlorine content, which could mitigate the aggressive deposit buildups generated in the reference line. The deposits containing a higher amount of chlorine would then remain on the outer part of all the deposits, making the path towards the material more intricate for corrosive species, i.e. chlorine. This agrees well with the chlorine content value (2.6% wt.) of the RecRef sample where only deposits from the outer part were analyzed, showing the high accumulation of chlorine in the outer part.

Reversely, the RefRec sample exhibited a higher material loss than the calculated mean value. This could be explained by the first buildup of deposits with high chlorine content from the harsh environment. Due to the hard deposits, even after placing the sample in a milder environment (Sulfur Recirculation), the corrosive species i.e. chlorine could remain active in the accelerated corrosion without being neutralized (e.g. via sulfation). Thus, the aggressiveness of the first layers of deposits building on a sample could dictate its future corrosion resistance.

3.3. Deposit/oxide microstructure

The Fig. 5 (a) illustrates the corrosion attack on the different sides of the ring after exposure in 2000 h in Ref (Ref). Most of the deposited/corrosion products spalled of during sample handling but some corrosion products can still be observed on both sides of the sample. The flue gas side exhibits in addition signs of steel grain boundaries attack.

The EDX analysis shown in Fig. 5 (b) shows that the corrosion products are mostly made of an outer chromium and iron-rich oxide. The nickel tends to stay in the inner oxide and at the interface metal/oxide or the corrosion front where the steel grain boundary attacks are located. No potassium was detected and only traces of sulfur were detected in good agreement with the IC results in

Indications of large amount of metal chlorides was observed at the interface metal/oxide which also correlates well with the IC results from the reference line (Fig. 2). The alloy grain boundary attack has been linked to the presence of large amount of KCl (Phother-Simon et al., 2020). This is in good agreement with the observed deposit/microstructure. The oxide microstructure indicates breakaway corrosion in line with earlier reports in KCl rich

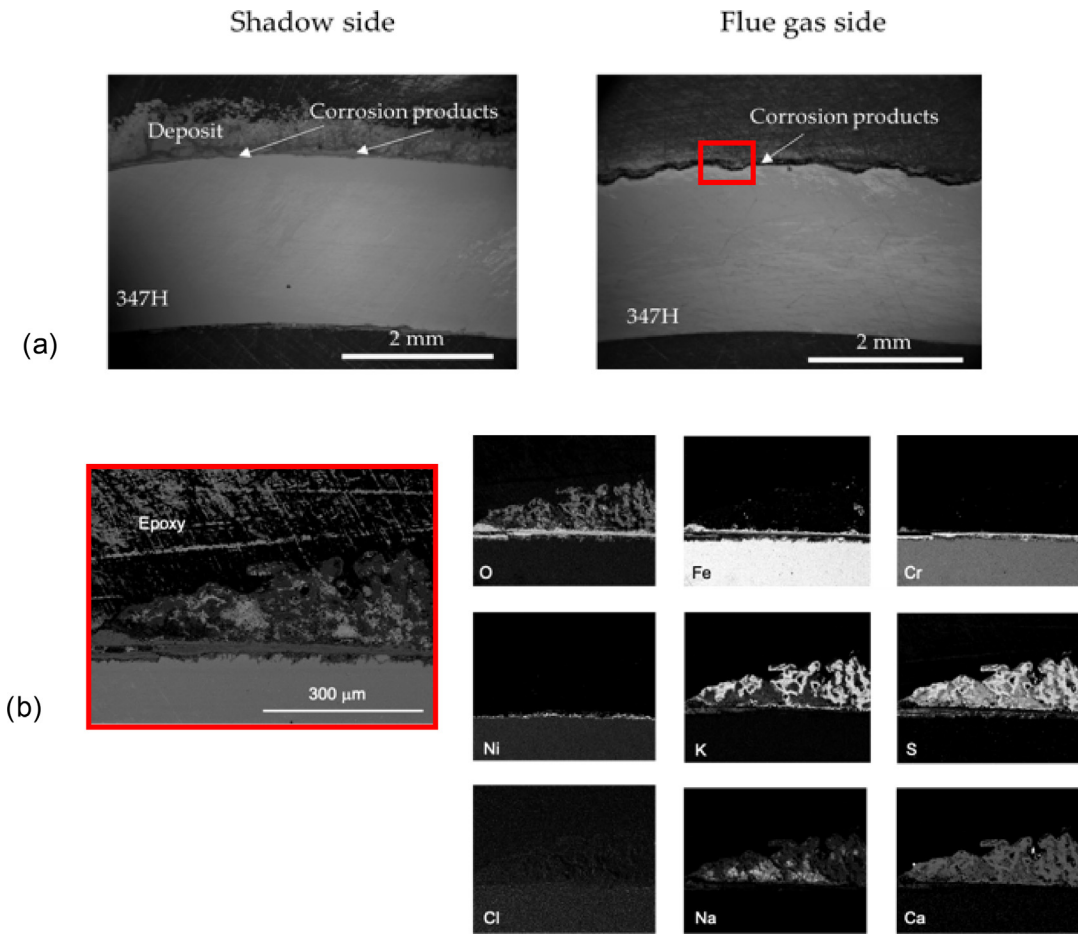

Fig. 6. (a) BSE image showing a low mag cross section side Rec for 2000 h (b) EDX analysis of the flue gas side of Rec for 2000 h.

environments (Karlsson et al., 2016; Phother-Simon, et al., 2020). The results in addition indicate a diffusion controlled grown scale with bad adhesion explaining the material loss.

The SEM images of the sample exposed in 1000 h Rec + 1000 h Rec (Rec) show a microstructure in good agreement with the overall thickness/material loss of the reference sample for the sulfur recirculation line Rec (Fig. 3). Small amounts of deposit remain on top of the shadow side while in the flue gas side case, it spalled off due to sample handling (Fig. 6 (a)). The material loss for Rec is lower than for Ref even on the flue gas side. No steel grain boundary attacks are observable for Rec as in the case for Ref (Fig. 6).

The EDX analysis presented in Fig. 6(b) shows a thin dense adherent oxide on the top of the sample mainly constituted of an outer iron rich layer above a chromium, nickel and iron (indicating a diffusion grown spinel) oxide. The oxide microstructure indicates breakaway oxidation, i.e. no signs of a thin protective chromium rich scale. The deposit remaining over the surface is mainly composed by calcium, potassium and sodium sulfates. These sulfates may be responsible for the hardness of the deposit. In concordance with the IC measurements no chlorine signal was detected along the interface metal/oxide.

In the case of the corrosion memory sample Rec Ref, some material loss could be observed on the flue gas side of the sample (Fig. 7), but less than the sample exposed only in the reference line (Ref). Most of the deposit spalled off due to sample handling but on some parts of the sample remains of deposit could be analyzed. The shadow side has a lower material loss, which is in agreement with the results shown in Fig. 3.

The EDX analysis presented in Fig. 7(b) shows that a layer of deposit mainly composed by sulfates. Due to the hardness of the deposit and the spallation during handling the samples, this deposit close to the sample surface corresponds only to the first 1000 h exposure in the sulfur recirculation line. The oxide scale has a similar microstructure as the Rec exposed sample, i.e. an iron rich oxide above a (Fe,Cr,Ni) oxide. There is no grain boundary attack and no/very small amounts of chlorine is detected in good agreement with the IC measurements (Fig. 2).

These results are in very good agreement with the material loss presented in Fig. 3 and Fig. 4 where it was shown that the Rec sample and the RecRef sample have a very similar material loss. The first 1000 h of exposure in the sulfur recirculation line seems to have a positive memory effect on the samples. A similar oxide scale microstructure could be observed despite 1000 h exposure in the more corrosive environment. Locally some thicker oxide scales could be observed while the microstructure has the same structure as the thinner parts (indications of a diffusion controlled grown microstructure). It may be noted that the inner part is richer in Cr (see Fig. 6(b)) indicating a healing layer slowing down the growth rate beneath the thicker oxide part. The less corrosive dense deposit in combination with the microstructure formed after breakaway caused by the presence of reactive alkali seems to protect the alloy for further corrosion during the second 1000 h exposure in the reference line.

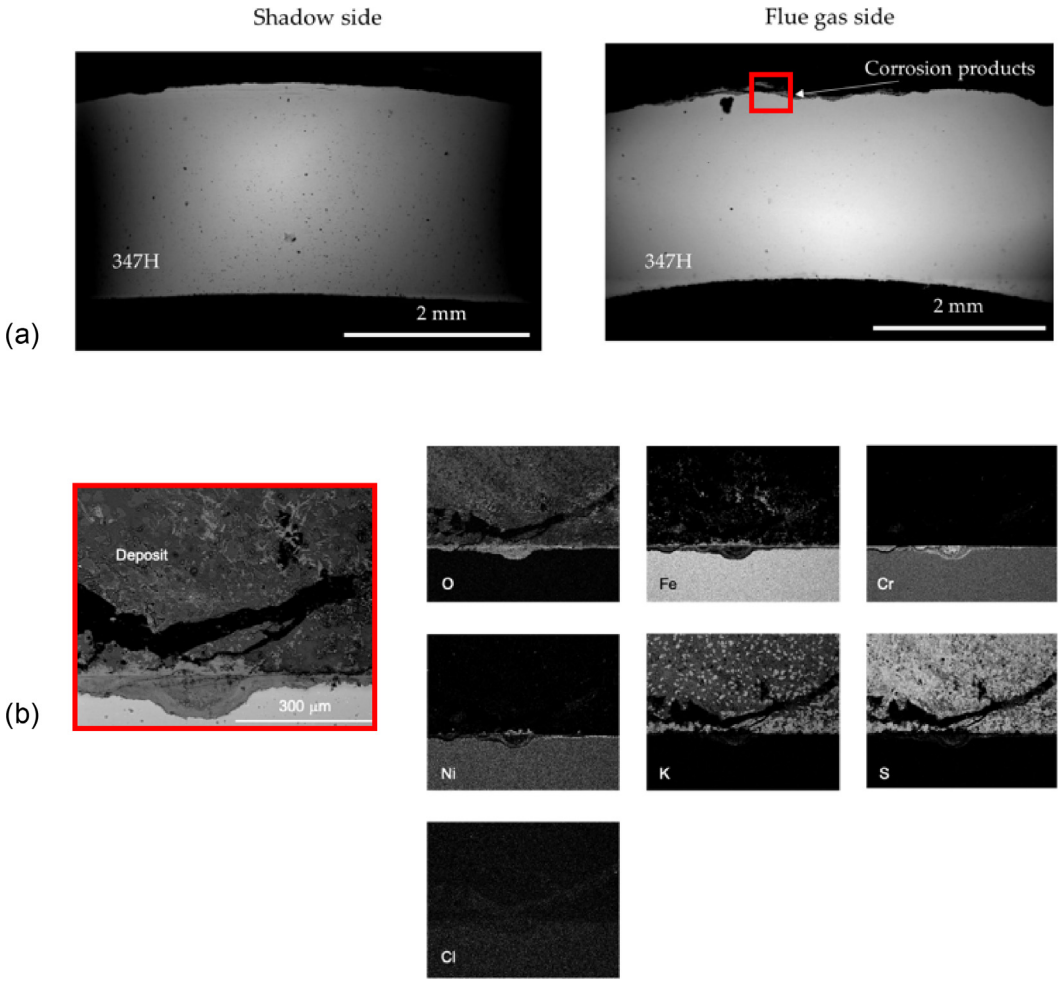

Fig. 7. (a) BSE image showing a high mag cross section of the Rec Ref for 2000 h (b) EDX analysis of the flue gas side of Rec Ref for 2000 h.

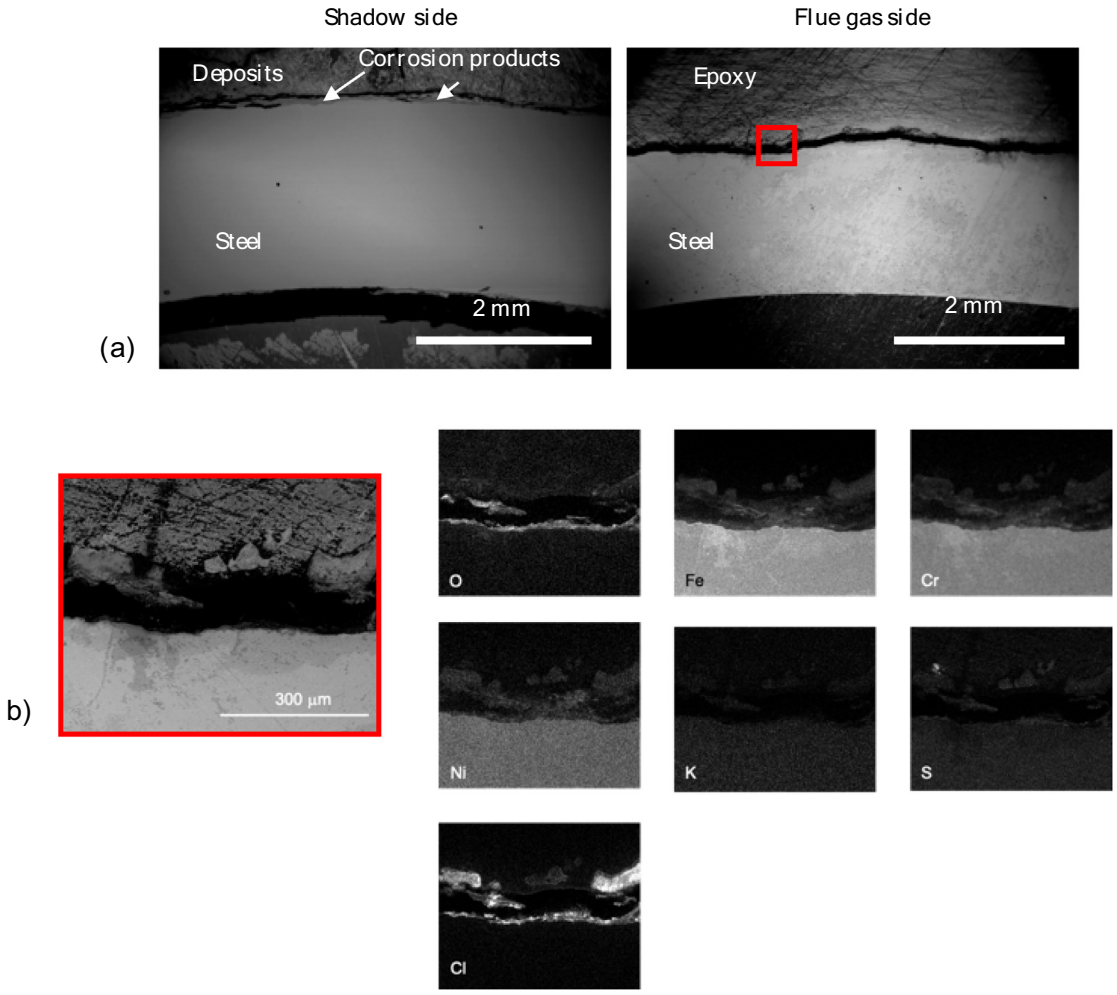

Fig. 8. (a) BSE image showing cross sections of the sample exposed in Ref Rec for 2000 h (b) SEM/EDX analysis of the flue gas side of Ref Rec for 2000 h.

In the other corrosion memory sample Ref Rec the sample was first exposed in a more corrosive environment for 1000 h. The material loss results indicated a strong memory effect and a corrosion attack in the same range as after 2000 h in the more corrosive environment (Ref). BSE images showing the sample Ref Rec are presented in Fig. 8. They show that the shadow side has remaining deposit on top of the oxide while on the flue gas side it has spalled off. The surface of the shadow side looks also smoother than the flue gas side and with less material loss, which agrees with the values presented in Fig. 3**.**

The EDX analysis presented in Fig. 8(b) shows a complex oxide scale with bad adhesion. A large amount of chlorine is also observed on top of the material, while no potassium and only traces of sulfur were observed. The oxide microstructure as well as the composition of the oxide and the amount of chlorine detected is very similar to the Ref sample **(**Fig. 2 and Fig. 6**(b)).** The remains from the corrosive environment, i.e. the non-protective oxide microstructure as well as the metal chlorides have a strong negative memory effect in the corrosion of the samples during the second 1000 h exposure in the sulfur recirculation line.

4. Conclusions

The full-scale Sulfur Recirculation technique installed in the CHP plant MEC changes the deposit chemistry and less corrosive species end up on the samples. This will result in less corrosion of the superheaters and formed a very good setting to simulate fuel variations in order to study possible corrosion memory effects.

The Corrosion Memory investigation shows that creating a less corrosive deposit initially may reduce corrosion in a more corrosive environment. However, the results also show that creating a corrosive deposit initially may increase the corrosion in a less corrosive environment. The results indicate that the memory effect is a combined influence of remaining deposit and the formed oxide microstructure.

Declaration of Competing Interest

The authors declare that they have no known competing financial interests or personal relationships that could have appeared to influence the work reported in this paper.

Acknowledgment

The Måbjerg Energy Center Waste to Energy plant is gratefully acknowledged for providing assistance during the tests. This work has been supported by KME (Cooperation Programme Materials technology) and Chalmers HTC (High Temperature Corrosion centre), financially supported by the Swedish Energy Agency and member companies.

Appendix A. Supplementary data

Supplementary data to this article can be found online at https://doi.org/10.1016/j.wasman.2021.05.005.

References

Abels, J.M., Strehblow, H.H., 1997. A surface analytical approach to the high temperature chlorination behaviour of inconel 600 at 700 °C. Corros. Sci. 39, 115–132. https://doi.org/10.1016/S0010-938X(96)00112-6.

Andersson, S., Blomqvist, E.W., Bafver, L., Jones, F., Davidsson, K., Froitzheim, J., Karlsson, M., Larsson, E., Liske, J., 2014. Sulfur recirculation for increased electricity production in Waste-to-Energy plants. Waste Manage. 34, 67–78. https://doi.org/10.1016/j.wasman.2013.09.002.

Andersson, S., Paz, M.D., Phother-Simon, J., Jonsson, T., 2019. High Temperature Corrosion and Dioxin Abatement Using Sulfur Recirculation in a Waste-to-Energy Plant. Detritus. 5, 92–98. https://doi.org/10.31025/2611-4135/2019.13784.

Cantatore, V., Olivas Ogaz, M.A., Liske, J., Jonsson, T., Svensson, J.-E., Johansson, L.-G., Panas, I., 2019. Oxidation Driven Permeation of Iron Oxide Scales by Chloride from Experiment Guided First-Principles Modeling. The Journal of Physical Chemistry C. 123, 25957–25966. https://doi.org/10.1021/acs.jpcc.9b06497.

Folkeson, N., Johansson, L.-G., Svensson, J.-E., 2007. Initial stages of the HCl-induced high-temperature corrosion of alloy 310. journal of the electrochemical society. 154, C515–C521.

Gerassimidou, S., Velis, C.A., Williams, P.T., Castaldi, M.J., Black, L., Komilis, D., 2020. Chlorine in waste-derived solid recovered fuel (SRF), co-combusted in cement kilns: A systematic review of sources, reactions, fate and implications. Critical Reviews in Environmental Science and Technology. https://doi.org/10.1080/10643389.2020.1717298.

Grabke, H.J., Reese, E., Spiegel, M., 1995. The effects of chlorides, hydrogen chloride, and sulfur dioxide in the oxidation of steels below deposits. Corros. Sci. 37, 1023–1043. https://doi.org/10.1016/0010-938X(95)00011-8.

Henderson, P., Szakalos, P., Pettersson, R., Andersson, C., Hogberg, J., 2006. Reducing superheater corrosion in wood-fired boilers. Materials and Corrosion-Werkstoffe Und Korrosion. 57, 128–134. https://doi.org/10.1002/maco.200503899.

Jonsson, T., Folkeson, N., Svensson, J.E., Johansson, L.G., Halvarsson, M., 2011. An ESEM in situ investigation of initial stages of the KCl induced high temperature corrosion of a Fe–2.25Cr–1Mo steel at 400°C. Corros. Sci. 53, 2233–2246. https://doi.org/10.1016/j.corsci.2011.03.007.

Karlsson, S., Åmand, L.-E., Liske, J., 2015. Reducing high-temperature corrosion on high-alloyed stainless steel superheaters by co-combustion of municipal sewage sludge in a fluidised bed boiler. Fuel 139, 482–493. https://doi.org/10.1016/j.fuel.2014.09.007.

Karlsson, S., Larsson, E., Jonsson, T., Svensson, J.E., Liske, J., 2016. A Laboratory Study of the in Situ Sulfation of Alkali Chloride Rich Deposits: Corrosion Perspective. Energy Fuels 30, 7256–7267. https://doi.org/10.1021/acs.energyfuels.6b00372.

Karlsson, S., Pettersson, J., Johansson, L.G., Svensson, J.E., 2012. Alkali induced high temperature corrosion of stainless steel: The influence of NaCl, KCl and CaCl 2. Oxid. Met. 78, 83–102. https://doi.org/10.1007/s11085-012-9293-7.

Karlsson, S., Pettersson, J., Svensson, J.E., Johansson, L.G., 2011. KCl-Induced high temperature corrosion of the austenitic stainless steel 304L - The influence of SO2. Journal. 696, 224–229. https://doi.org/10.4028/www.scientific.net/MSF.696.224.

Krause, H.H., Vaughan, D.A., Boyd, W.K., 1975. Corrosion and Deposits from Combustion of Solid-Waste. 3. Effects of Sulfur on Boiler Tube Metals. Journal of Engineering for Power-Transactions of the Asme. 97, 448–452. https://doi.org/10.1115/1.3446029.

Ma, W.C., Wenga, T., Frandsen, F.J., Yan, B.B., Chen, G.Y., 2020. The fate of chlorine during MSW incineration: Vaporization, transformation, deposition, corrosion and remedies. Prog. Energy Combust. Sci. 76. ARTN 100789.

McNallan, M., Liang, W., Kim, S., Kang, C., 1983. Acceleration of the high temperature oxidation of metals by chlorine. Journal.

Meissner, T.M., Montero, X., Fahsing, D., Galetz, M.C., 2020. Cr diffusion coatings on a ferritic-martensitic steel for corrosion protection f in KCl-rich biomass co-firing environments. Corros. Sci. 164. ARTN 108343.

Nielsen, H.P., Frandsen, F.J., Dam-Johansen, K., Baxter, L.L., 2000. The implications of chlorine-associated corrosion on the operation of biomass-fired boilers. Prog. Energy Combust. Sci. 26, 283–298. https://doi.org/10.1016/S0360-1285(00)00003-4.

Paz, M.D., Jonsson, T., Liske, J., 2018a. Testing of new materials to combat superheater corrosion in waste fired CFB boiler. South Korea.

Paz, M.D., Olivas Ogaz, M.A., Jonsson, T., Petterson, A., Moradian, F., Jonasson, A., Aspen, J., Schneider, P., Mahanen, J., Vänskä, K., Barisic, V., Jönsson, B., Hernblom, J., Huhtakangas, M., Liske, J., 2018b. Combating high temperature corrosion by new materials and testing procedures - The effect of increased fractions of waste wood on water wall and superheater corrosion. Report KME.

Paz, M.D., Zhao, D., Karlsson, S., Liske, J., Jonsson, T., 2017. Investigating corrosion memory: The influence of previous boiler operation on current corrosion rate. Fuel Process. Technol. 156, 348–356. https://doi.org/10.1016/j.fuproc.2016.09.018.

Paz, M. D. J., T.; Liske,J.; Karlsson,S.; Davis,C.; Jonasson,A.; Sandberg,T., 2014. Study of corrosion memory in boiler heat surfaces by field tests with biomass fuel mixes including sulphur and refuse fractions.

Pettersson, J., Folkeson, N., Johansson, L.G., Svensson, J.E., 2011. The effects of KCl, K 2SO 4 and K 2CO 3 on the high temperature corrosion of a 304-type austenitic stainless steel. Oxid. Met. 76, 93–109. https://doi.org/10.1007/s11085-011-9240-z.

Phother-Simon, J., Jonsson, T., Liske, J., 2020. Continuous KCl addition in high temperature exposures of 304 L - A way to mimic a boiler environment. Corros. Sci. 167. ARTN 108511.

Reddy, L., Sattari, M., Davis, C.J., Shipway, P.H., Halvarsson, M., Hussain, T., 2019. Influence of KCl and HCl on a laser clad FeCrAl alloy: In-Situ SEM and controlled environment High temperature corrosion. Corros. Sci. 158. https://doi.org/10.1016/j.corsci.2019.07.003.

Shinata, Y., 1987. Accelerated oxidation rate of chromium induced by sodium chloride. Oxid. Met. 27, 315–332. https://doi.org/10.1007/BF00659274.

Vainio, E., Demartini, N., Hupa, L., Amand, L.E., Richards, T., Hupa, M., 2019. Hygroscopic Properties of Calcium Chloride and Its Role on Cold-End Corrosion in Biomass Combustion. Energy Fuels 33, 11913–11922. https://doi.org/10.1021/acs.energyfuels.9b02731.

Vainio, E., Yrjas, P., Zevenhoven, M., Brink, A., Lauren, T., Hupa, M., Kajolinna, T., Vesala, H., 2013. The fate of chlorine, sulfur, and potassium during co-combustion of bark, sludge, and solid recovered fuel in an industrial scale BFB boiler. Fuel Process. Technol. 105, 59–68. https://doi.org/10.1016/j.fuproc.2011.08.021.

Viklund, P., Pettersson, R., Hjornhede, A., Henderson, P., Sjovall, P., 2009. Effect of sulphur containing additive on initial corrosion of superheater tubes in waste fired boiler. Corros. Eng., Sci. Technol. 44, 234–240. https://doi.org/10.1179/174327809x419203.

Vinter Dahl, K., Montgomery, M., Chekol Malade, Y., Grumsen, F., Aakjae Jensen, S., Mikkelsen, L., Hauris Jespersen, O., Peder Hansen, N., Andersson, S., Paz, M.D., Jonsson, T., Phother-Simon, J., Liske, J., 2018. Sulfur recirculation and improved material selection for high temperature corrosion abatement. Report KME.

Wagner, C., 1933. Beitrag zur Theorie des Anluafvorgangs. Physicalische Chemie. 21B, 25–41.

Wang, C.-J., He, T.-T., 2002. Morphological Development of Subscale Formation in Fe–Cr–(Ni) Alloys with Chloride and Sulfates Coating. Oxid. Met. 58, 415–437. https://doi.org/10.1023/A:1020119107724.

Zahs, A., Spiegel, M., Grabke, H.J., 2000. Chloridation and oxidation of iron, chromium, nickel and their alloys in chloridizing and oxidizing atmospheres at 400–700°C. Corros. Sci. 42, 1093–1122. https://doi.org/10.1016/S0010-938X(99)00142-0.